SECURITY CLASSIFICATION OF THIS PAGE

REPORT DOCUMENTATION PAGE

1a. REPORT SECURITY CLASSIFICATION: Unclassified	1b. RESTRICTIVE MARKINGS
2a. SECURITY CLASSIFICATION AUTHORITY	3. DISTRIBUTION/AVAILABILITY OF REPORT: Approved for public release; distribution unlimited
2b. DECLASSIFICATION/DOWNGRADING SCHEDULE	
4. PERFORMING ORGANIZATION REPORT NUMBER(S): Technical Report # 6	5. MONITORING ORGANIZATION REPORT NUMBER(S)
6a. NAME OF PERFORMING ORGANIZATION: Materials Engineering Dept. RPI; 6b. OFFICE SYMBOL (If applicable)	7a. NAME OF MONITORING ORGANIZATION: Office of Naval Research
6c. ADDRESS (City, State and ZIP Code): Troy, NY 12180-3590	7b. ADDRESS (City, State and ZIP Code): Chemistry Program, 800 N. Quincy Street, Arlington, VA 22217
8a. NAME OF FUNDING/SPONSORING ORGANIZATION: Office of Naval Research; 8b. OFFICE SYMBOL (If applicable)	9. PROCUREMENT INSTRUMENT IDENTIFICATION NUMBER: Contract # N00014-86-K-0259
8c. ADDRESS (City, State and ZIP Code): Chemistry Program, 800 N. Quincy St., Arlington, VA 22217	10. SOURCE OF FUNDING NOS.

PROGRAM ELEMENT NO.	PROJECT NO.	TASK NO.	WORK UNIT NO.
NR	056	533	

11. TITLE (Include Security Classification): THE KINETICS AND MECHANISM OF OXYGEN UPTAKE ON A POLYCRYSTALLINE IRON SURFACE

12. PERSONAL AUTHOR(S): Mehran Arbab and John B. Hudson

13a. TYPE OF REPORT	13b. TIME COVERED	14. DATE OF REPORT (Yr., Mo., Day)	15. PAGE COUNT
Interim Technical	FROM 3/1/86 TO 2/28/88	1988-2-28	39

16. SUPPLEMENTARY NOTATION: To be published in Surface Science

17. COSATI CODES			18. SUBJECT TERMS (Continue on reverse if necessary and identify by block number)
FIELD	GROUP	SUB. GR.	Surfaces, chemistry, kinetics, adsorption, oxygen, metals
Surface	Reactions		

19. ABSTRACT (Continue on reverse if necessary and identify by block number)

The initial uptake of oxygen has been studied on a clean, polycrystalline iron surface over the temperature range between 360 and 575 K, using a combination of Auger electron spectroscopy and mass spectrometry. An initial chemisorption period is followed in turn by a temperature dependent linear oxidation regime and a final period of decreasing oxidation rate. Chemisorption kinetics can be explained by an intrinsic molecular precursor mechanism. The linear oxidation period involves uptake into the near-surface bulk by a non-activated place exchange mechanism.

20. DISTRIBUTION/AVAILABILITY OF ABSTRACT	21. ABSTRACT SECURITY CLASSIFICATION
UNCLASSIFIED/UNLIMITED ☒ SAME AS RPT. ☐ DTIC USERS ☐	unclassified

22a. NAME OF RESPONSIBLE INDIVIDUAL	22b. TELEPHONE NUMBER (Include Area Code)	22c. OFFICE SYMBOL
Dr. David L. Nelson	(202) 698-4410	

DD FORM 1473, 83 APR — EDITION OF 1 JAN 73 IS OBSOLETE.

OFFICE OF NAVAL RESEARCH

Contract N00014-86-K-0259

Task No. NR-056-533

TECHNICAL REPORT NO. 6

THE KINETICS AND MECHANISM OF OXYGEN UPTAKE ON A POLYCRYSTALLINE IRON SURFACE

BY

Mehran Arbab* and John B. Hudson
Materials Engineering Department
Rensselaer Polytechnic Institute
Troy, NY 12180-3590

*Present Address:
Materials Engineering Department
Case Western Reserve University
Cleveland, OH 44106

Accession For	
NTIS GRA&I	☒
DTIC TAB	☐
Unannounced	☐
Justification	
By	
Distribution/	
Availability Codes	
Dist	Avail and/or Special
A-1	

February 28, 1988

ABSTRACT

The initial uptake of oxygen has been studied on a clean, polycrystalline iron surface over the temperature range between 360 and 575 K, using a combination of Auger electron spectroscopy and mass spectrometry. An initial chemisorption period is followed in turn by a temperature dependent linear oxidation regime and a final period of decreasing oxidation rate. Chemisorption kinetics can be explained by an intrinsic molecular precursor mechanism. The linear oxidation period involves uptake into the near-surface bulk by a non-activated place exchange mechanism.

1- INTRODUCTION:

Many studies of oxygen adsorption on iron have been performed. They include adsorption on the (100) [1-9], (110) [9-16], and polycrystalline [9,17] surfaces, as well as thin films [18-20]. In general, these studies show the same sequence of events: Oxide formation is preceded by the chemisorption of oxygen [1,3,4,7,8,11]. Under ultrahigh vacuum conditions, and at room temperature or below, up to a few monolayers of the oxide form (the uhv limit of oxide thickness), suggesting that the initial oxidation process may be only slightly activated [1,3,4,7,10,11]. To gain more insight into this process, we have studied the influence of the substrate temperature on oxygen adsorption on a polycrystalline iron surface. Two earlier studies of this effect report conflicting results: Leygraf and Ekelund [9] report that oxygen adsorption occurs more rapidly at 400 K than at 300 K, for both (100) and (110) surfaces of iron. On the other hand , Sewell et al. [6] observed no measurable temperature dependence, in the 298-423 K range, on the (100) surface.

A more recent study [7] has considered the effect of temperature on the reconstruction of the oxide phase formed by room temperature exposure of an Fe(100) surface to oxygen until the uhv limit of oxide thickness was reached. This oxide is a disordered phase, as determined by LEED [4] and Low energy ion scattering (LEIS) [7]. Annealing the oxidized sample in the 573-643 K range resulted in a significant reconstruction of the oxide, without any measurable oxygen desorption. LEIS experiments that followed the adsorption or anneal periods indicated the rearrangement of oxygen in the subsurface region, with a significant amount of oxygen, about one monolayer, remaining on the top of the surface. The above study determined

that the reconstruction of the oxide formed at room temperature is an activated process. However, the question of the formation of the thin disordered oxide phase remains.

A number of uhv studies performed at room temperature show that the rate of post-chemisorption oxygen uptake remains independent of the amount of adsorbed oxygen up to exposures of about 20 L or higher [1,2,10], i.e. the sticking coefficient remains constant with time (in a number of these studies the transition from chemisorption to oxide formation is characterized by a minimum in the sticking coefficient vs coverage curve). Fehlner and Mott [21], in a review of the early evidence for this apparently coverage-independent adsorption process, proposed an explanation. They suggested that the adsorption of oxygen into a molecular state is followed by its dissociation into adsorbed atomic oxygen species, which are in turn incorporated into the oxide phase by a non-activated place exchange with the surface metal atoms. Various possible explanations of the origin of the zero or small activation energy associated with this exchange process have been proposed [21-23,41]. We will examine the above model in view of our experimental results which, unlike those available to Fehlner and Mott, were performed on clean surfaces. Also, based on a review of the available literature, a model will be proposed to account for the transition from chemisorption to initial oxide formation.

2. EXPERIMENTAL:

A detailed description of the apparatus used in this study has been presented elsewhere [24]. Briefly, the all stainless steel ultrahigh vacuum system was comprised of two chambers, which were interconnected

through a 1.45 mm diameter orifice. The main chamber was equipped with a cylindrical mirror electron energy analyzer with a co-axial electron gun for Auger electron spectroscopy (AES), an ion gun for sputter cleaning of the sample surface, and the sample manipulator. A base pressure of 5 x 10^{-10} torr could be attained after bake out. The detector chamber housed a quadrupole mass spectrometer (QMS) and was independently evacuated to a base pressure of better than 2 x 10^{-10} torr (ionization gauge limit).

The polycrystalline iron sample was an integral part of a permeation cell which was used for hydrogen permeation [24] and oxygen titration studies [25]. The high purity, 1 mm thick iron sample (MARZ Grade, Materials Research Corporation) was TIG welded to the low carbon steel cell. The sample was heated by electron bombardment from the backside. Its temperature was monitored by a W-5%Re, W-26%Re thermocouple spot welded near the front of the cell. The surface of the sample was cleaned by the now conventional method applied to iron surfaces - i.e. repeated cycles of argon ion sputtering and annealing in vacuum-until the coverage of all surface contaminants were reduced to at most a few atomic percent, as determined by AES. The large mass of the permeation cell resulted inevitably in slow cooling rates after anneal. This limited the lowest temperature to which a sample could be cooled without being appreciably contaminated by the background gases to about 375 K in most instances.

Optical microscopy of the sample after the completion of experiments showed it to be comprised of coarse grains, about 20% of which had average diameters of 1 mm or larger. An average ASTM grain size of 5 was estimated for the specimen. Laue x-ray diffraction patterns taken on various spots on the sample indicated no preferred orientation. In one

instance, diffraction from one or more of the larger grains resulted in a well defined pattern characteristic of a high index plane (a (429) orientation). The (429) plane can be envisaged as (001) terraces separated by (210) steps, where for monatomic step heights the terraces will be alternatively 4 and 5 atomic rows wide, the rows defining the <120> direction. The (210) orientation may in turn be thought of as regularly spaced (100) steps and (010) kinks.

Gases were admitted to the main chamber via leak valves. Partial pressures were measured by an ionization gauge calibrated according to the manufacturer's specifications. In the case of oxygen, and particularly at pressures exceeding 10^{-8} torr, this method was observed to be unreliable and often to result in the overestimation of the partial pressure. Therefore, the QMS was calibrated against the ionization gauge at pressures below 10^{-8} torr, where the correspondence between the outputs of the two instruments was linear, and was subsequently employed for P_{O2} measurements. While utilizing the mass spectrometer for this purpose results in a precise determination of the relative changes in the partial pressure of oxygen, the accuracy in absolute partial pressure measurements will continue to depend on the sensitivity of the ionization gauge, and the extent of backstreaming of other gasses from the ion pump, at low presssures.

The oxygen coverage on the iron surface was followed by measuring the ratio of the height of the instantaneous oxygen KLL peak (503eV), I_O, to that of the iron LMM peak (703eV), I_{Fe}, as measured on a clean surface prior to each run. This ratio, which we shall refer to as I^* hereafter, was not independently calibrated, but it was assumed [26] to be proportional to the oxygen coverage on the sample surface, θ :

$$I^* = I_O / I_{Fe} = \beta \cdot \Theta \ , \qquad (1)$$

where β is an undetermined constant of calibration. All Auger spectra were obtained using a 6 eV peak to peak modulation of the CMA pass voltage, except for the fine structure analysis of the 47 eV Auger peak of iron, where a 1 eV modulation was used.

3- RESULTS:

3.1- Oxygen uptake kinetics

Oxygen adlayer coverage as a function of exposure at 360 K (the lowest temperature at which an experiment was performed) is shown in Figure 1. The oxygen concentration is plotted in terms of I^*, the ratio of the oxygen Auger peak height to that of iron, as explained above. Three regions of oxygen adsorption were generally distinguishable. Fast initial adsorption of oxygen, region I in Figure 1, is followed by a period of linear oxygen uptake (region II) after 2-2.5 L of exposure. For 15L and higher, a nonlinear regime (region III), with a decreasing rate of uptake, characterized the adsorption behavior and continued for exposures of 100L and more.

The iron MVV Auger transition appears at 47 eV (dN(E)/dE mode) [26]. The peak shape associated with this transition has been frequently reported to undergo changes with oxygen exposure (ref. 15 and the references therein). A low energy shoulder has been observed to appear near the positive peak of the Auger feature as the chemisorbed oxygen is incorporated into an initial oxide phase. Thus, in order to distinguish between the different adsorption regimes, the variations in the fine structure of this peak were recorded for a number of I^* values. Typical

examples are shown in Figure 2. The intensity of the 47 eV peak was observed to decrease rapidly with increasing oxygen coverage. This peak was eventually replaced by another peak at approximately 43 eV for $I^*>1$. In addition to the above changes, the magnitude of a high energy shoulder, present even in the structure of the MVV transition peak of a clean surface, was seen to increase gradually with coverage. Unlike the low energy shoulder at 43 eV, which is generally attributed to oxide formation, the origin of the high energy shoulder at about 52 eV is still unclear [3,4].

The oxide peak, clearly visible at $I^*=0.26$, first became discernible at $I^*\sim0.21$. The iron MVV peak retained its initial structure for I^* smaller than 0.17, except for the aforementioned decrease in its intensity and some broadening of the positive peak. Thus, oxidation first begins in the $0.17<I^*<0.21$ range and continues thereafter.

Seo et al. [27] have studied the structure of the MVV Auger peak of iron for its various oxides and have tabulated the relative positions in energy of the three distinct features associated with this Auger transition. A comparison of the present data on the energy of the iron oxide peak with their reference data reveals the oxidized iron to be triply ionized (γ-Fe_2O_3). Sakisaka et al. [1] and Miyano et al. [10] found that room temperature oxidation of Fe(100) results in a similar state of oxidation (γ-Fe_2O_3), while oxidation of Fe(110) results in a doubly ionized state (FeO). In this respect, our polycrystalline sample resembles the (100) surface of iron in its oxygen adsorption behavior.

Returning to Figure 1, the three oxygen adsorption regimes may now be attributed to chemisorption in region I and oxidation in regions II and III. The boundaries separating these regions may be only broadly defined

at this time.

This behavior is similar to that observed previously in studies of the Fe(100) surface, but differs in several respects from previous studies on the Fe(110) surface. In the case of Fe(110), two distinct chemisorption regimes are observed [e.g. 12], rather than the single one observed in the present work and for Fe(100) substrates [1-4]. The interaction between adsorbed oxygen and hydrogen resulted in incomplete titration in the sample studied in the present work [25], as has also been observed for the Fe(100) surface [28]. Similar studies on the Fe(110) surface [29], on the other hand, showed complete titration.

The effect of substrate temperature on the adsorption kinetics is shown in Figure 3, for exposures up to 40 L. The overall adsorption behavior is in all cases similar to that observed at 360 K. While the rate of oxygen uptake remains independent of temperature in region I of adsorption (chemisorption), the uptake rate during the initial (linear) oxidation period decreases with increasing temperature.

Assuming that oxygen, once adsorbed, does not desorb (see below), and that I^* is proportional to the oxygen coverage on the surface, the slopes of the uptake curves in Figures 1 and 3 are proportional to the sticking coefficient of oxygen on iron. Thus the sticking coefficient in the chemisorption region is found to be independent of the substrate temperature, while in the subsequent linear uptake region an inverse dependence of this parameter on the substrate temperature is observed. The sticking coefficient in the third region of oxide growth was found to decrease as the amount of oxygen adsorbed on the surface was increased. In contrast to region II, the rate of decrease in the sticking coefficient in this case was slower at 550 K than at 360 K, indicating a thermally activated process. However, due to the finite inelastic mean free path

(IMFP) of the Auger electrons and the resulting complications arising from the attenuation of the Auger electon intensity for thicker oxide overlayers, a detailed kinetic analysis in the third region was not attempted.

High temperature adsorption studies were complicated by the dissolution of oxygen into the bulk of the substrate (to a region beyond the IMFP of the Auger electrons), as indicated by an isothermal decrease in I^* after the removal of gaseous oxygen. The attribution of the disappearance of the adsorbed oxygen to its dissolution was confirmed by heating a pre-exposed substrate. While the magnitude of I^* decreased with time for temperatures exceeding 550 K, no O_2 evolution was detected by the QMS. This is in agreement with the work of Vink et al. [7] on the Fe(100) surface. They observed that annealing an oxidized surface results in a reconstruction of the subsurface oxide, leading to a drop in the Auger parameter, without any oxygen desorption, for T>643 K.

In the temperature and pressure ranges of interest and for coverages within the linear oxidation region, the extent of oxygen dissolution into regions too deep for detection by AES was small relative to the adsorption rate. Detailed experiments on the titration of adsorbed oxygen by hydrogen, carried out in a separate study, showed that the total amount of water formed in the 575-625 K range was nearly temperature independent [25]. Furthermore, the titration rate, as measured by AES, and the water formation and desorption rates, as determined by mass spectrometry, were identical for T<625 K. This indicates that the thickness of the oxygenated overlayer, at least up to the onset of the third adsorption period, does not significantly attenuate the oxygen KLL Auger intensity (See below).

The effect of oxygen partial pressure on the rate of oxygen uptake in the linear adsorption period was also studied. The results obtained at 375 K are shown in Figure 4. In the indicated range, the adsorption rate was observed to vary linearly with P_{O2}.

3.2- Oxygen coverage calibration

A plot of the 47 eV iron MVV Auger peak intensity for various oxygen exposures, normalized with respect to the intensity of the clean iron LMM peak, conforms to the expected exponential attenuation behavior for $I^*<0.8$ (Figure 5). The IMFP of the 47 eV Auger electron during both oxygen chemisorption on and oxidation of iron has been measured to be 4.7 A° [30]. These results may be used to establish a relationship between the parameter I^* and the thickness of the surface oxygenated layer. According to Figure 5, the Auger peak is reduced by a factor of 1/e at I^* - 0.44. These values indicate an effective thickness of 1.8-2.2 A° ($0.17<I^*<0.21$) for the inelastic scattering of the Auger electrons by the chemisorbed layer formed prior to the onset of oxidation. In Section 4.3 it will be argued that this chemisorbed layer is almost saturated prior to the onset of oxidation and remains stable on the surface during the formation of the two dimensional oxide phase. On this basis, the thickness of the oxide formed on the top of the iron substrate at the end of the linear adsorption period is determined to be between 3.6 and 4.1 A°.

By comparing AES and ellipsometry during oxygen uptake experiments, Vink et al. [7] have found that, due to the finite IMFP of the Auger electrons, the normalized oxygen Auger peak is proportional to oxygen concentration only up to an oxygenated overlayer thickness of 8-9 A°. For

thicker oxides, the inelastic scattering of the Auger electrons becomes significant. According to the present calibration, this thickness corresponds to an average I^* value of 0.8, in good agreement with Figure 5, where for $I^*>0.8$ the actual near surface oxygen concentration is clearly underestimated by the attenuated oxygen Auger signal.

The above information provides a basis for determining the pre-oxidation coverage of chemisorbed oxygen. γ-Fe_2O_3 has a spinel structure with a lattice constant of 8.32 A° [31]. This corresponds to an anion concentration of 5.56×10^{14} cm^{-3}. If it is assumed that the two dimensional oxide formed on our polycrystalline sample has a stoichiometry equivalent to bulk γ-Fe_2O_3, the above calibration translates into an oxygen concentration of 5.9×10^{15} to 6.0×10^{15} cm^{-3} when $I^*=1.0$. Hence, for a planar density of 1.21×10^{15} adsorption site/cm^3 (the average density on the (110), (100), and (111) planes, or on the (100) plane alone) the oxygen coverage corresponding to $0.17<I^*<0.21$ is between 0.8 and 1.0 monolayers. Obviously this calibration procedure is only approximate. However, it is noteworthy that the final result is in good agreement with many studies on Fe(100) [2,6-8], which have also concluded a coverage of one monolayer for pre-oxide oxygen chemisorption at room temperature.

4- DISCUSSION:

Analysis of the experimental data is complicated by the fact that the sample studied was polycrystalline and consequently a range of crystallographic orientations contributed to the observed results; previous studies on the (110) and (100) surface of iron have shown that

oxygen adsorption is strongly orientation-dependent. In spite of this, as described above, many aspects of oxygen adsorption and titration on this sample are very similar to those observed on Fe(100). This is not too surprising since at least one of the larger grains was identified as having the (429) orientation, which is a surface vicinal to the (100) plane (Section 2). Therefore, in the following sections, when appropriate and for the sake of simplicity, we will assume that the sample has a (100) geometry. The discussion, however, will remain general.

4.1- Chemisorption:

As shown by the variations in the fine structure of the iron MVV Auger peak, oxidation begins within the $0.17<I^{*}<0.21$ range. The chemisorption period is characterized by a temperature-independent, approximately linear decrease of the oxygen uptake rate, i.e., dI^{*}/dt, with I^{*}. The high initial sticking coefficient of oxygen on iron films at a temperature as low as 195 K [20] suggests non-activated chemisorption. In addition, the sticking coefficient has been found to decrease more slowly with coverage than expected from the Langmuir dissociative adsorption model [20,4]. Thus, the dissociative chemisorption of oxygen [3,11] appears to be preceded by a precursor state. In accordance with these observations, Simmons and Dwyer [4] proposed a model which is also in good agreement with our results. They assumed a mobile molecular precursor to the chemisorption of oxygen, which adsorbs only on sites unoccupied by the chemisorbed atomic species and which rapidly assumes a small steady state concentration. This model leads to the following expression for the sticking coefficient [4]:

$$S = \frac{a(1-\theta)}{1+\frac{k_d}{K_a}(1-\theta)^2}, \qquad (2)$$

where a is the trapping probability for the precursor, and k_d and k_a are the specific rate constants for its desorption and dissociation into chemisorbed oxygen atoms, respectively. For k_d/k_a small compared to unity (in the temperature range of $300<T(K)<575$ as far as the present study is concerned), the above expression yields a linear dependence of the sticking coefficient on $(1-\theta)$.

A fit of the uptake rate versus coverage data for $I^*<0.17$, by the least square method, to $S = \{1-(I^*/I^*_{sat})\}$, is shown in Figure 6. The fitting parameter, I^*_{sat}, which corresponds to the oxygen coverage of the saturated chemisorbed overlayer, is 0.21 ± 0.01. This value is in good agreement with the transition range of I^* determined in Section 3, and, according to the calibration described in that section, corresponds to about one monolayer of adsorbed oxygen. The initially high value of the sticking coefficient in region I may be due to the direct dissociative chemisorption of gaseous oxygen molecules at the surface defects, including steps and kinks, that exist on the surface of our sample.

It is necessary to note that the direct dissociation mechanism (i.e. Langmuir model) is also insensitive to the substrate temperature. The Langmuir model is, however, incapable of explaining the entire chemisorption regime in this study; its application to the present data predicts a chemisorbed saturation coverage within region II of adsorption (i.e. corresponding to oxide growth).

4.2- The initial oxidation:

The initial oxidation of iron was characterized by a sticking coefficient independent of the instantaneous oxygen coverage. The sticking coefficient did, however, decrease by more than one order of magnitude as the substrate temperature was raised from 360 to 575 K. Furthermore, the uptake rate was directly proportional to the oxygen partial pressure.

Following the early work of Fehlner and Mott [21], we propose the following scheme to account for the above observations. The incorporation of the newly-adsorbed oxygen atoms into the initial oxide phase is assumed to occur normal to the surface of the adsorbent. Such an incorporation will result in the regeneration of the adsorption site, which will be re-occupied when a molecular precursor encounters two such sites that are adjacent to each other. These assumptions agree well with the experimental results of Dorfeld et al. [13] regarding the adsorption of oxygen on the Fe (110) surface . It was found that an interruption in the supply of gaseous oxygen during the post-chemisorption period resulted in no change in the total amount of the adsorbed oxygen, determined by AES. However, upon the re-introduction of gas-phase oxygen, adsorption took place at an enhanced rate; the magnitude of the sticking coefficient at a given coverage was significantly greater than that for the uninterrupted-exposure experiment. Therefore, new adsorption sites must have formed in the absence of gas-phase oxygen. Due to the short lifetime of a weakly bound precursor state (about 1 microsecond [4]) relative to the gas interruption intervals (several minutes [13]) site regeneration in the absence of gas-phase oxygen can not be attributed to a process which involves the precursor state. Horgan and King [20], conducted similar gas interruption experiments on deposited films of iron and other metals.

They concluded that site regeneration occurs by the incorporation of a strongly bound oxygen species into the oxide layer. Some of their experiments were performed at temperatures as low as 195 K. This, along with the expected high activation energy for oxygen surface diffusion, suggest that the incorporation process is a local phenomenon and procedes, as proposed by Dorfeld et al. [13], by the incorporation of the adsorbed species normal to the surface.

A final, and yet perhaps the most important, assumption concerning the linear oxidation model is that the incorporation of the chemisorbed species into the metal substrate is a non-activated process (see Section 4.3). Since the incorporation process, or the regeneration of the adsorption site, is assumed to be non-activated, it occurs as soon as an oxygen atom is chemisorbed (in a time comparable to the vibrational frequency of the adsorbed species [21]). Therefore, the coverage of the oxide forming sites remains constant with time, for the duration of this period. These assumptions lead to the following adsorption-oxidation sequence:

$$O_{2,g} \underset{k'_d}{\overset{a'Z}{\rightleftarrows}} O_{2,P'} \xrightarrow{k'_a} 2O_{ox}, \qquad (3)$$

where Z is the O_2 impingement rate, and a', k'_a, and k'_d are the trapping probability and the dissociation and desorption rate constants for the molecularly adsorbed species, respectively. As will be explained in Section 4.5, after a large fraction of the chemisorption sites have become occupied, oxygen will adsorb primarily on a second type of surface site, prior to becoming incorporated into the oxide phase. On the (100)

surface of iron, for example, this second adsorption site could be the on-top sites in contrast to the four-fold hollow sites occupied by chemisorbed oxygen [2,8]. In expression 3, O_{ox} represents the oxygen species adsorbed on such sites as well as those already in the oxide phase. Again, as in the previous case, the absence of any oxygen desorption upon heating an oxidized substrate leads us to assume that oxygen, once dissociated, does not recombine to form O_2. Similar to the case of chemisorption, we will make the steady state approximation [32] in regards to the population of the precursor states, [P'], which yields:

$$[P'] = \frac{a'Z}{k'_d+k'_a} \quad . \tag{4}$$

The rate of oxygen adsorption in this period can be now written as:

$$\frac{d[O_{ox}]}{dt} = SZ = \frac{2a'Z}{1+(k'_d/k'_a)}. \tag{5}$$

The expression for the sticking coefficient is thus:

$$S = \frac{2a'}{1+(k'_d/k'_a)} \quad . \tag{6}$$

The change in I^* with time will thus be:

$$\frac{dI^*}{dt} = \frac{b}{1+(k°'_d/k°'_a)\exp(-\Delta H_p'/RT)} \quad , \tag{7}$$

where b is a constant that includes the gas-phase impingement rate, the Auger calibration factor, and the trapping probability; $\Delta H_p'$ is the

difference in the activation energies for dissociation and desorption of the precursor ($\Delta H'_d - \Delta H'_a$), and $k^{\circ\prime}_d$ and $k^{\circ\prime}_a$ are the corresponding frequency prefactors.

The experimental values of dI^*/dt were obtained by linear regression analysis of the linear portion of the uptake curves of Figure 3 and are shown, together with their corresponding 95% confidence limit, in Figure 7. Also shown in this figure is a least squares fit of expression 7 to the data. This fitting procedure yields a value of 10.0 Kcal/mole for $\Delta H_p'$, in very good agreement with the minimum value of 9.0 Kcal/mole predicted by Simmons and Dwyer [4] for the adsorption energy of the precursor to chemisorption and oxide formation. The value of the frequency prefactor ratio, i.e. $k^{\circ\prime}_d/k^{\circ\prime}_a$, was found to be 2.8×10^4. Simmons and Dwyer [4], using transition state theory, have found a corresponding value of approximately 1.2×10^6 at 300 K, in good agreement with our experimentally determined value.

Following the linear uptake range, the value of dI^*/dt decreased as I^* increased, suggesting that the regeneration of the adsorption sites was no longer a non-activated process. Moreover, the rate of decrease was slower at higher temperatures, also indicating an activated process.

The result of the linear oxidation period, observed in several studies, is the formation of a two-dimensional oxide which precedes bulk oxide formation [1,4]. Holloway and Hudson [33] have observed temperature effects on the rate of oxygen uptake by Ni(100) and Ni(111) surfaces which are analogous to the present study. While the sticking coefficient was found to be independent of temperature during the chemisorption period, it decreased with increasing temperature during the initial oxidation stage.

These authors deduced a different oxidation mechanism for the rapid uptake period. The variation in the sticking coefficient with oxygen coverage in that work was characteristic of the nucleation and growth of two-dimensional oxide islands. A similar mechanism was inferred by Simmons and Dwyer [4] for the initial oxidation of an Fe(100) surface. The island mechanism, however, does not describe the linear adsorption kinetics observed in this, and other [21,10,2], studies, nor does it explain the regeneration of the adsorption sites in the absence of gaseous oxygen [13, 20].

4.4- Non-activated oxygen incorporation:

All observations made in this study - the coverage-independent character of the sticking coefficient, its decrease as the substrate temperature is increased, and the first order dependence of the oxygen uptake rate on oxygen partial pressure- are accounted for by the above oxygen incorporation model. A similar scheme was originally proposed, on the basis of the early results on the low temperature oxidation of different metals, by Fehlner and Mott [21]. Later studies of oxygen adsorption on clean iron single crystals have also produced kinetic results which may be explained on the basis of the above model. That is, the initial oxidation period, mainly at room temperature, has been observed to proceed linearly.

Despite much kinetic evidence in support of this apparently non-activated oxygen incorporation process, a viable explanation of the phenomenon is still unavailable. In their paper, Fehlner and Mott [21] proposed that the initial oxidation occurs by a direct adatom-metal atom

place exchange. The expected high activation energy for such a place exchange was proposed to be compensated by an image force energy due to the interaction of the negatively-charged chemisorbed oxygen with the metal substrate. This energy, which was calculated to be large for oxide layers less than a few monolayers thick, decreases in magnitude as the thickness of the oxide is increased, until the net activation energy becomes positive and the oxidation kinetics become non-linear. Depending on the metal substrate, the linear oxidation behavior can be observed up to a few monolayers.

This model has been cited in the literature without a critical examination [e.g. 1,34,41]. For a 2 A° movement of the charged species, Fehlner and Mott [21] calculated that this force will translate into a net gain in energy of about 50 Kcal/mole; large enough to compensate for the activation energy of the place-exchange process, which would presumably be of the order of the energy required for breaking a bond between a metal atom and the bulk (about 50 Kcal/mole for iron). Consequently, the apparent activation energy will be small or zero until the oxide thickness exceeds a critical value. Unfortunately, Fehlner and Mott [21] did not explicitly indicate the assumed magnitude of the negative charge on the chemisorbed oxygen. We can only assume that, in order to arrive at 50 Kcal/mole, they must have taken it to be equivalent to a large fraction of the unit electronic charge ($\approx \frac{1}{2}e$).

The existing data on the increase in the work function of iron due to oxygen adsorption suggest that the above assumption is an overestimate of the extent of charge transfer during chemisorption. A number of independently performed studies have shown that the maximum increase in the electron work function of iron, during the oxygen chemisorption

period, is of the order of 0.25-0.6 eV [1,3,10,12]. If we assume that the adsorption geometry on Fe(100) is that deduced by Legg et al. [2] and recently confirmed by Van Zoest et al. [8], that the chemisorption coverage at saturation is 0.5 ML, and that all the first neighbor iron atoms, in both the first and second metal layers, contribute equally to the chemisorption bond, and use the Helmholtz equation for work function calculations [35], we find only 3-7% of a unit of charge transferred to each chemisorbed oxygen atom. (The coverage at saturation of chemisorbed oxygen on Fe(100) has been variably reported as 0.5 [4] or 1 monolayer [7]. Choosing 0.5 ML in the above calculation can only overestimate the extent of charge transfer to the adsorbate.) This finding is in good agreement with the calculations of Van Hove [35] for oxygen chemisorption on nickel and tungsten. Therefore, A 2 A° movement of the chemisorbed atom within the corresponding electrostatic field will result in an effective decrease in energy of about 1 Kcal/mole, which is substantially less than that calculated by Fehlner and Mott.

Other mechanisms have been suggested. Delchar et al. [22] have proposed that the incorporation of chemisorbed oxygen, located in a four-fold hollow site, is assisted by the concerted outward movement of the four neighboring metal atoms on the surface. They have calculated that this process has a small, but finite, probability. The interstitial penetration of the adsorbate, however, does not result in the regeneration of adsorption sites; a condition required by the present kinetic model. It has also been proposed that the heat of adsorption of the molecular species may assist the activated incorporation of the adsorbed species [23].

Clearly, none of the above hypotheses are independently capable of

explaining the incorporation phenomenon. A combined process may be operative.

4.5- The onset of oxidation:

According to Figure. 3, the oxidation process does not begin before a certain chemisorbed oxygen coverage is formed (see Section 2). A number of previous studies on this adsorption system [2-4] and others [21,36], are in agreement with this observation.

The various states of oxygen adsorbed on a metal surface may be more clearly distinguished using high resolution electron energy loss spectroscopy (HREELS). Erley and Ibach [11] applied this method to the adsorption of oxygen on Fe(110). A loss feature attributed to chemisorbed oxygen appeared on the spectrum in the 500-550 cm^{-1} range. The intensity of this feature increased with the amount of oxygen adsorbed, for exposures up to 6L. For exposures of 7L and higher, a second feature, around 400 cm^{-1}, emerged on the spectrum. This peak, whose intensity increased with higher exposures, can be attributed to oxygen incorporated into the subsurface region of the Fe(110) substrate. Of central significance to the present discussion is that the loss feature at 550 cm^{-1} remained unchanged both in intensity and frequency for up to 20L of exposure, i.e. well into the oxidation period, at which point the intensity of the 400 cm^{-1} loss feature surmounted it.

Furthermore, according to oxygen adsorption experiments of Legg et al. [2], the p(1x1) monolayer of oxygen adsorbed on the surface of Fe(100) at room temperature remains stable for periods of up to eight hours. Van Zoest et al. [8] also examined the adsorption geometry of oxygen on both

clean and oxidized Fe(100) surfaces. The samples were exposed to oxygen until either one monolayer of adsorbed oxygen or the uhv limit of the oxide thickness was obtained (Section. 1). On both surfaces, annealing resulted in the p(1x1) surface structure, which for both specimens is associated with one monolayer of oxygen adsorbed on the top of the surface [7,8]. LEIS experiments showed that on both surfaces oxygen occupies the four-fold hollow sites and is at the same elevation relative to the plane of the first iron atom layer, suggesting similar interactions of the chemisorbed oxygen with the top iron layer, regardless of the presence or absence of oxygen in the subsurface region.

Therefore, for the two single crystal surfaces of iron that have been studied, i.e. the (110) and (100) surfaces, the existing evidence suggests that the overlayer formed during the chemisorption period saturates prior to, and remains stable during, further oxygen uptake, and that there is little change in the local bonding of the chemisorbed species due to further oxygen uptake. Similar observations have been made for other metal-oxygen systems [37].

A possible explanation may be given on the basis of the findings of Fisher and Schmieg [38] on the surface of another group VIII metal. These authors combined thermal desorption spectroscopy with isotope exchange experiments to study the different states of adsorbed oxygen on the Rh(100) surface. The four thermally-induced desorption peaks due to atomically adsorbed oxygen species included the high temperature β_4 state at low coverages and the low temperature β_1 state at high coverages. For exposures at 100 K, and only for oxygen coverages beyond half a monolayer, a molecularly adsorbed species was also observed to desorb. In addition, the atomic β_1 state, whose appearance the above

authors attributed to the onset of oxide formation, was observed to form only in association with the molecular state, i.e. the molecular state is the precursor to this species. The formation of this species was observed only for T<250 K, perhaps due to the small residence time of the molecular state. The authors also inferred the existence of a precursor to the formation of the β_4-β_2 states [38].

These observations suggest that the β_2-β_4 states form preferentially upon oxygen-exposure, due to either thermodynamic or kinetic reasons, and that a measurable suface concentration of the precursor to the β_1 state can develop only when these phases approach saturation. That is, formation of the β_1 phase (the onset of oxidation) takes place only at sites where the precursor cannot take the easier (or more favorable) route to the chemisorbed state. It is also possible that two types of molecular species can exist on the surface with different bonding characteristics and energies. In fact, on the Pt(111) surface, two distinct forms of associatively adsorbed oxygen species have been observed by HREELS [39]; while the population of one predominates at low (dissociated) oxygen coverages that of the other increases monotonically at higher coverages [40].

On the basis of the above arguements, we propose that the population of the molecular precursor, [P'], to the adsorption of oxygen into the initial oxide phase, O_{ox}, may be a function of the chemisorbed oxygen coverage, θ_c. In this case, the adsorption sequence shown in Equation 3 may be rewritten as:

$$O_{2,g} \underset{k'_d}{\overset{a'Zf(\theta_c)}{\rightleftharpoons}} O_{2,P'} \xrightarrow{k'_a} 2O_{ox} \quad . \tag{8}$$

In the absence of direct information on $f(\theta_c)$, we will assume that the precursor has a finite lifetime only at points where incorporation into the chemisorbed layer is impossible - e.g. at iron sites completely surrounded by chemisorbed oxygen, which, for cubic symmetry leads, to $f(\theta_c)= \theta_c^4$. Assuming that oxygen chemisorption on the (100) surface proceeds according to $(1-\theta_c)$ kinetics (Section 4.1 and Reference 4), θ_c as a function of time, t, may be written as:

$$\theta_c = 1-X \qquad (9)$$

where $X=\exp(-2aZt/N_o)$.

The expression for the rate of change in the surface coverage of O_{ox}, following reaction scheme 8 (see also Section 3.2.1) is thus

$$\frac{d[O_{ox}]}{dt} = SZ = \frac{2a'Z\theta_c^4}{1+(k'_d/k'_a)} . \qquad (10)$$

Substituting for θ_c from expression 9 and integrating, we obtain:

$$\theta_{ox} = \frac{AZ}{N_o}\left[t + \frac{N_o}{2aZ}\left(4X-3X^2-\frac{4}{3}X^3-\tfrac{1}{4}X^4-\frac{25}{12}\right)\right] \qquad (11)$$

where $A= \dfrac{2a'}{1+\dfrac{k_d'}{k_a'}}$, and X has its previous meaning.

Since AES does not allow us to distinguish between O_c and O_{ox}, the total "coverage" must be considered. The stability of the chemisorbed

oxygen, as discussed above, leads us to assume that, except for the effect of the chemisorbed oxygen on the adsorption of the molecular precursor to oxide formation, uptake into the two states of oxygen proceeds independently; that is, the two processes are additive. Indeed there may be a contribution to θ_c from the dissociation of the molecular species on sites neighbouring unoccupied chemisorption sites. However, the population of this molecular state becomes significant only for large values of θ_c, where the fraction of the unoccupied chemisorption sites is small. Therefore this contribution will be assumed to be small. Hence, the overall sticking coefficient may be expressed as:

$$S=\frac{N_o}{Z} \cdot \frac{d\theta}{dt} = S_c + S_{ox} \qquad (12)$$

The oxygen uptake rates, plotted as dI^*/dt versus I^*, where dI^*/dt was obtained by differentiating the uptake curves of Figure 3, are shown in Figure 8 for all temperatures studied. The data obtained at 360, 475, and 575 K, normalized to the value of dI^*/dt observed at $I^* = 0$, are compared to the results expected from Equation 12 in Figure 9. In developing this figure, the initial sticking coefficient was arbitrarily chosen as unity, while the initial oxidation parameters were taken from Section 4.2 above. The agreement between the predicted and experimental profiles is quite good, especially at lower temperatures. At higher temperatures, the model overestimates the rate of decrease in S just prior to the plateau. Results for the measurements at other temperatures showed similar agreement, but are not shown on Figure 9 for clarity. In the preceding formulation, the value of k_d/k_a (Equation 2) was assumed to be small enough to allow for the approximation of the RHS of Equation 2 as

$S_o(1-\theta_c)$. For larger values of the above parameter, this approximation is not valid as θ_c approaches unity. In that case, a minimum in the sticking coefficient profile will appear before a plateau is realized; the depth below the plateau and the coverage range of this minimum will depend on the magnitude of k_d/k_a. Minima of varying prominence, perhaps due to the sensitivity of k_d/k_a to the surface structure, have been observed to precede the plateaus in the sticking coefficient of oxygen on iron in a number of previous studies [1,3,4].

5- Summary:

The results of oxygen adsorption measurements on a polycrystalline iron surface, at substrate temperatures ($360<T(K)<575$) can be summarized as follows:

1-The initial chemisorption of oxygen is independent of the substrate temperature. The kinetics of adsorption in this period are consistent with a model that involves a molecular precursor state which adsorbs only on sites unoccupied by the chemisorbed species.

2-The rate of oxygen uptake in the oxidation period immediately following chemisorption is independent of coverage, but increases linearly with oxygen partial pressure, and decreases with increasing substrate temperature.

3-The initial oxidation can be explained in terms of the incorporation of the adsorbed oxygen atoms through a process which results in the regeneration of the adsorption sites involved (e.g. by place exchange). This process is assumed to be non-activated. The dissociative

adsorption step is preceded by a molecular precursor.

4-The experimental data, when fitted to the above model, indicate that the heat of adsorption of the oxygen molecule exceeds the activation energy for the dissociation of the precursor by 10 Kcal/mole.

5-The delayed oxidation of iron, also noted in a number of previous studies, can be explained in terms of the incorporation process being limited to those oxygen species adsorbed on sites different from the normal chemisorption sites. That is, oxygen adsorbed on a chemisorption site is a more stable species than either the oxide anion or the oxygen species adsorbed on other surface sites. Hence, the oxidation rate becomes significant only when a large fraction of the chemisorption sites have become occupied.

Acknowledgements:

This work was supported in part by ARO under Contract No. DAAL003-86-K-0076, and in part by the chemistry program of ONR. This support is gratefully acknowledged. The work is based on a thesis presented by one of us (M.A.) in partial fulfillment of the requirements for the Ph.D. degree at Rensselaer Polytechnic Institute.

FIGURE CAPTIONS:

Figure 1 Oxygen uptake at 360 K; region I: chemisorption, regions II and III: oxidation.

Figure 2 Iron MVV Auger peak at various oxygen coverages (I^*). The peak intensity is in arbitrary units with similar scale for all spectra.

Figure 3 Oxygen uptake at various substrate temperatures: ●, 360 K; ▲, 475 K; Δ, 525 K.

Figure 4 The rate of adsorption during the linear oxidation period (region II in Figure 1) versus oxygen partial pressure at a temperature of 375 K.

Figure 5 The intensity of the iron MVV Auger peak, I^*MVV (arbitrary units), versus I^*. Note that the exponential fit to the data (the solid line) becomes inadequate for $I^*>0.8$.

Figure 6 The rate of adsorption during the chemisorption stage: ●, 360 K; ○, 425 K; ▲, 475 K; Δ, 525 K; ■, 550 K; □, 575 K. I^*_f is the amount of oxygen which remains on the surface after the titration of the oxidized surface by hydrogen [25]. The solid line is the fit of data to the model discussed in Section 4.2.

Figure 7 The rate of oxygen uptake during the linear oxidation period (region II in Figure 1) at different substrate temperatures. The error bars indicate the 95% confidence limit on the data points. The solid line shows the fit of the proposed model to data.

Figure 8 Oxygen uptake rate, dI^*/dt vs coverage, I^*, obtained by differentiation of the coverage vs time data as shown in Figure 3: ●, 360 K; ○, 425 K; ▲, 475 K; △, 525 K; ■, 550 K; □, 575 K.

Figure 9 Oxygen sticking coefficient vs. coverage. The experimental data are normalized with respect to the value of dI^*/dt at $I^*=0$, which was evaluated by extrapolation from Figure 6. The value of I^* corresponding to 1 ML, is as determined in Section 3: ●, 360 K; ▲, 475 K; □, 575 K; Solid lines are fits of the data to Equation 12, using Equations 2 and 11.

REFERENCES:

[1] Y. Sakisaka, T. Miyano, and M. Onchi, Phys. Rev. B, 30 (1984) 6849.

[2] K. O. Legg, F. Jona, D. W. Jepsen, and P. M. Marcus, Phys. Rev. B, 16 (1977) 5271.

[3] C. F. Brucker and T. N. Rhodin, Surface Sci. 57 (1976) 523.

[4] G. W. Simmons and D. J. Dwyer, Surface Sci. 48 (1975) 373.

[5] A. J. Pignocco and G. E. Pellissier, J. Electrochem. Soc. 112 (1965) 1188.

[6] P. B. Sewell, D. F. Mitchell, and M. Cohen, Surface Sci. 33 (1972) 535.

[7] T. J. Vink, J. M. Der Kinderen, O. L. J. Gijzeman, J. W. Geus, and J. M. Van Zoest, Appl. Surface Sci. 26 (1986) 357.

[8] J. M. Van Zoest, J. M. Fluit, T. J. Vink, and B. A. Van Hassel, Surface Sci. 182 (1987) 179.

[9] C. Leygraf and S. Ekelund, Surface Sci. 40 (1973) 609.

[10] T. Miyano, Y. Sakisaka, T. Komeda, and M. Onchi, Surface Sci. 169 (1986) 197.

[11] W. Erley and H. Ibach, Sol. State Comm. 37 (1981) 937.

[12] G. Pirug, G. Broden, and H. P. Bonzel, Surface Sci. 94 (1980) 323.

[13] W. G. Dorfeld, J. B. Hudson, and R. Zuhr, Surface Science, 57 (1976) 460.

[14] A. J. Melmed and J. J. Carroll, J. Vac. Sci. Technol. 10 (1973) 164.

[15] K. Moliere and F. Portele, in The Structure and Chemistry of Solid Surfaces, Ed. G. A. Somorjai (1968) 69-1.

[16] A. J. Pignocco and G. E. Pellissier, Surface Sci. 7 (1967) 261.

[17] G. Ertl and K. Wandelt, Surface Sci., 50 (1975) 479.

[18] G. Alshorachi and G. Wedler, Appl. Surface Sci. 20 (1985) 279.

[19] M. Suleman and E. B. Pattison, Surface Sci. 35 (1973) 75.

[20] A. M. Horgan and D. A. King, Surface Sci. 23 (1970) 259.

[21] F. P. Fehlner and N. F. Mott, Oxid. Met. 2 (1970) 59.

[22] T. A. Delchar and F. C. Tompkins, Proc. Roy. Soc. (London), 300A (1967) 141.

[23] M. A. H. Lanyon and B. M. W. Trapnell, Proc. Roy. Soc. (London) A227 (1955) 387.

[24] M. Arbab and J. B. Hudson, Appl. Surface Sci. 29 (1987) 1.

[25] M. Arbab and J. B. Hudson, to be published.

[26] L. E. Davis, N. C. McDonald, P. W. Palmberg, G. E. Riach, and L. E. Weber, Handbook of Auger Electron Spectroscopy, 2nd ed., (1976, Physical Electronics).

[27] a- M. Seo, J. B. Lumsden, and R. W. Staehle, Surface Sci. 42 (1974) 337;

b- M. Seo, J. B. Lumsden, and R. W. Staehle, Surface Sci. 50 (1975) 541.

[28] T. J. Vink, J. M. Der Kinderen, O. L. J. Gijzeman, J. W. Geus, and J. M. Van Zoest, Appl. Surface Sci. 26 (1986) 357.

[29] T. J. Vink, S. J. M. Sas, O. L. J. Gijzeman, and J. W. Geus, J. Vac. Sci. Technol. A5 (1987) 1028.

[30] P. B. Needham Jr. and T. J. Driscoll, J. Vac. Sci. Technol. 11 (1974) 278.

[31] R. T. Phelps, E. A. Gulbransen, and J. W. Hickman, Ind. Eng. Chem., Anal. ed. 18 (1946) 391.

[32] R. Gorte and L. D. Schmidt, Surface Sci. 102 (1981) 388.

[33] a- P. H. Holloway and J. B. Hudson, Surface Sci. 43 (1974) 123;
b- P. H. Holloway and J. B. Hudson, Surface Sci. 43 (1974) 141.

[34] M. W. Roberts and C. S. McKee, Chemistry of Metal-Gas Interface (1978, Oxford Univ. Press).

[35] M. A. Van Hove, in The Nature of The Surface Chemical Bond, Ed. T. N. Rhodin and G. Ertl (1979, North-Holland).

[36] C. R. Brundle and J. Q. Broughton, in The Chemical Physics of Solid Surfaces and Heterogeneous Catalysis, vol. 3, Ed. D. A. King and D. P. Woodruff, to be published.

[37] J. L. Gland, B. A. Sexton, and G. B. Fisher, Surface Sci. 95 (1980) 587.

[38] G. B. Fisher and S. J. Schmieg, J. Vac. Sci. Technol. A (1983) 1064.

[39] S. Lehwald, H. Ibach, and H. Steininger, Surface Sci. 117 (1982) 342.

[40] N. R. Avery, Chem. Phys. Lett. 96 (1983) 371.

[41] K. R. Lawless, Reports on Progress in Physics 37 (1974) 231.

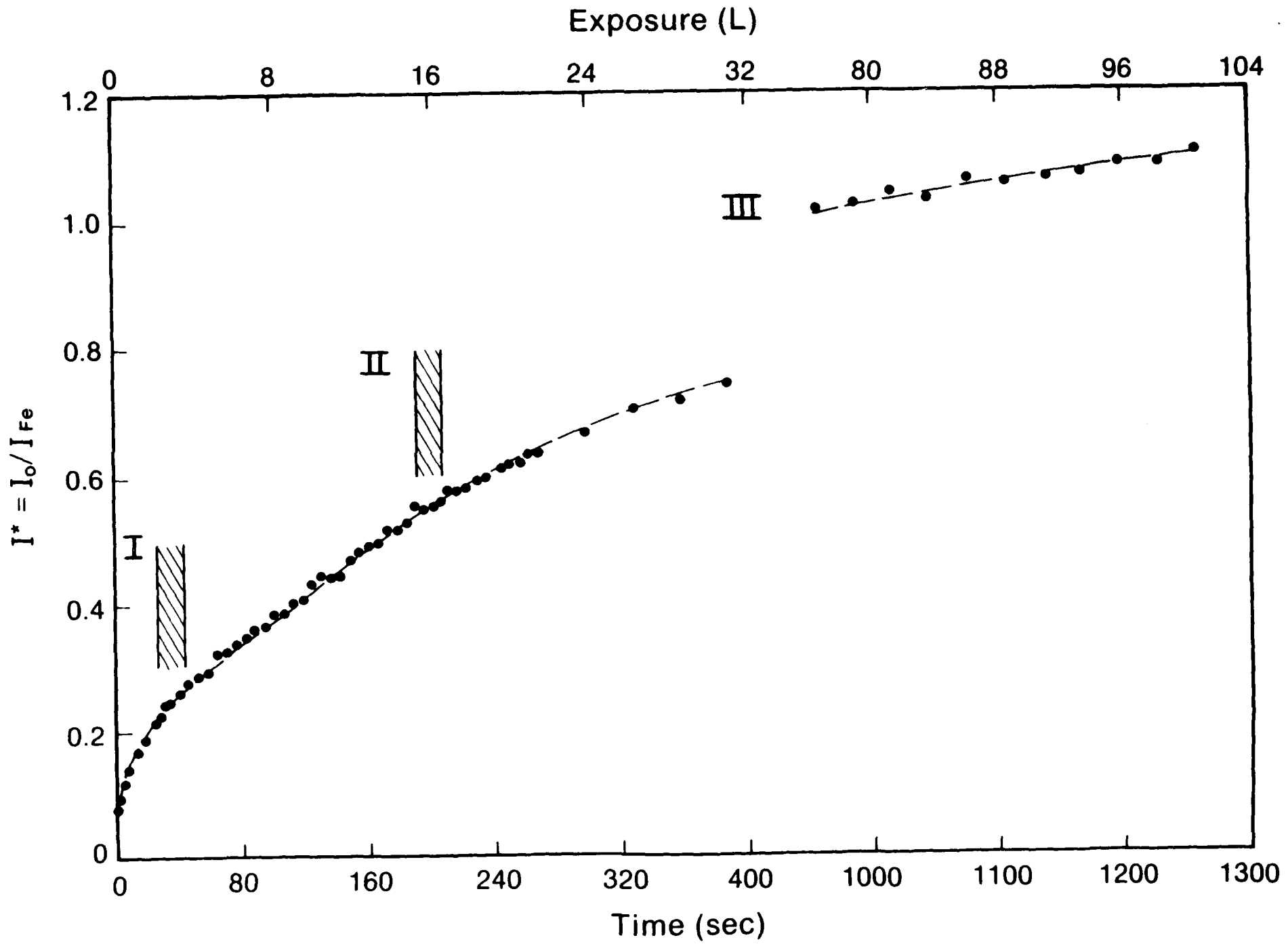
Exposure (L)
0
8
16
24
32
80
88
96
104
1.2
1.0
0.8
0.6
0.4
0.2
0
$I^* = I_o / I_{Fe}$
I
II
III
0
80
160
240
320
400
1000
1100
1200
1300
Time (sec)

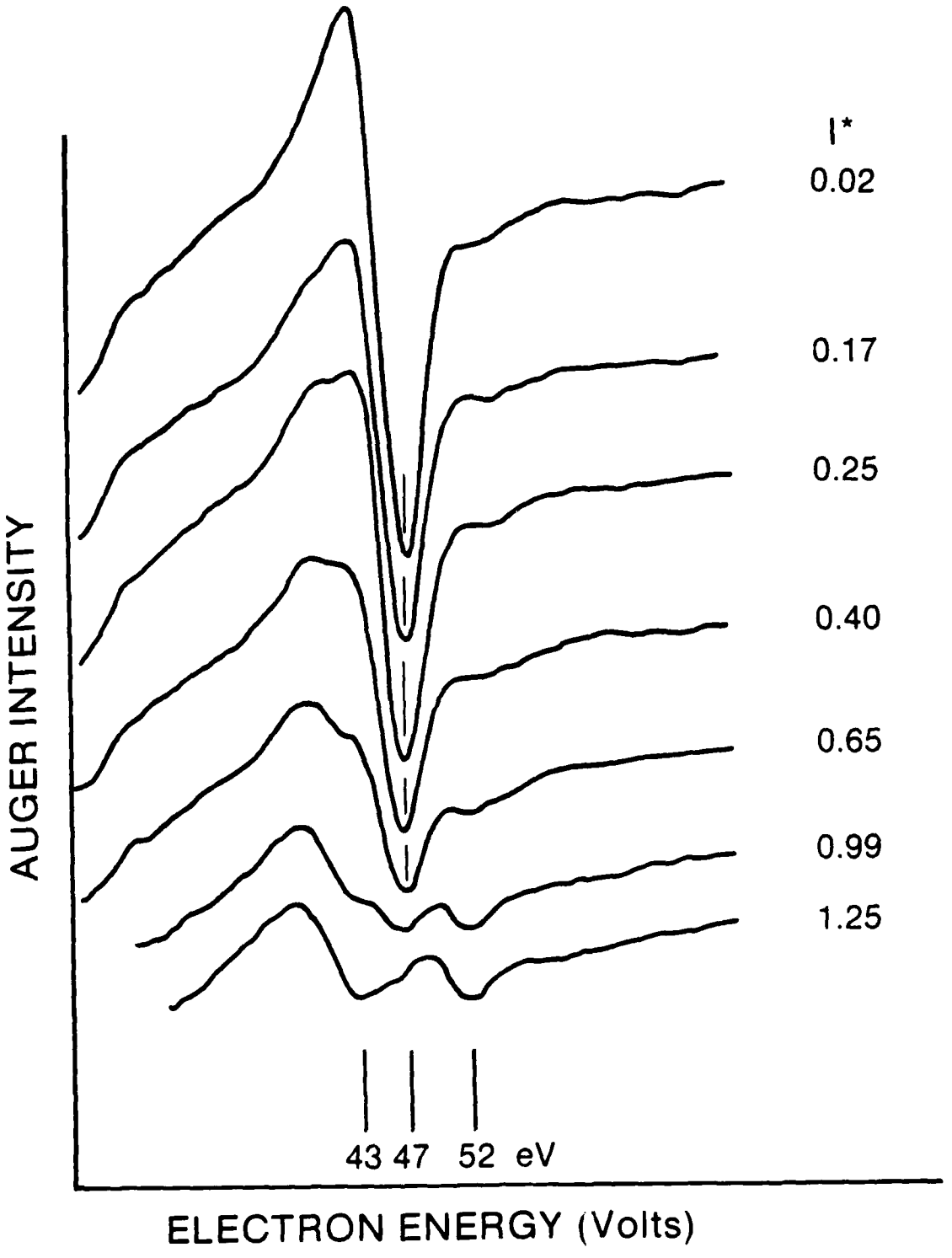
I*
0.02
0.17
0.25
0.40
0.65
0.99
1.25
AUGER INTENSITY
43 47 52 eV
ELECTRON ENERGY (Volts)

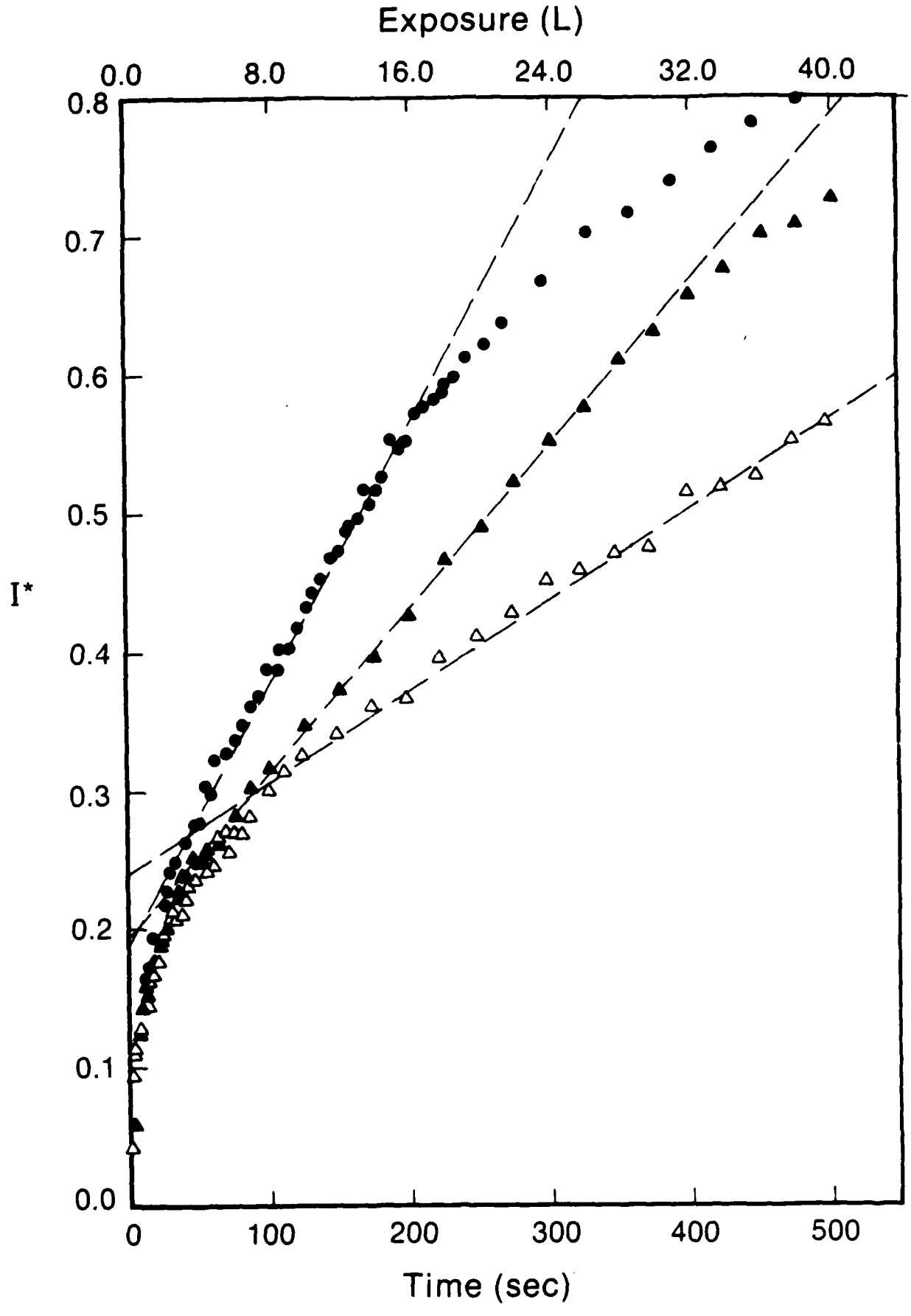

FIGURE 3 M. ALGARNI & J. M. HUDSON

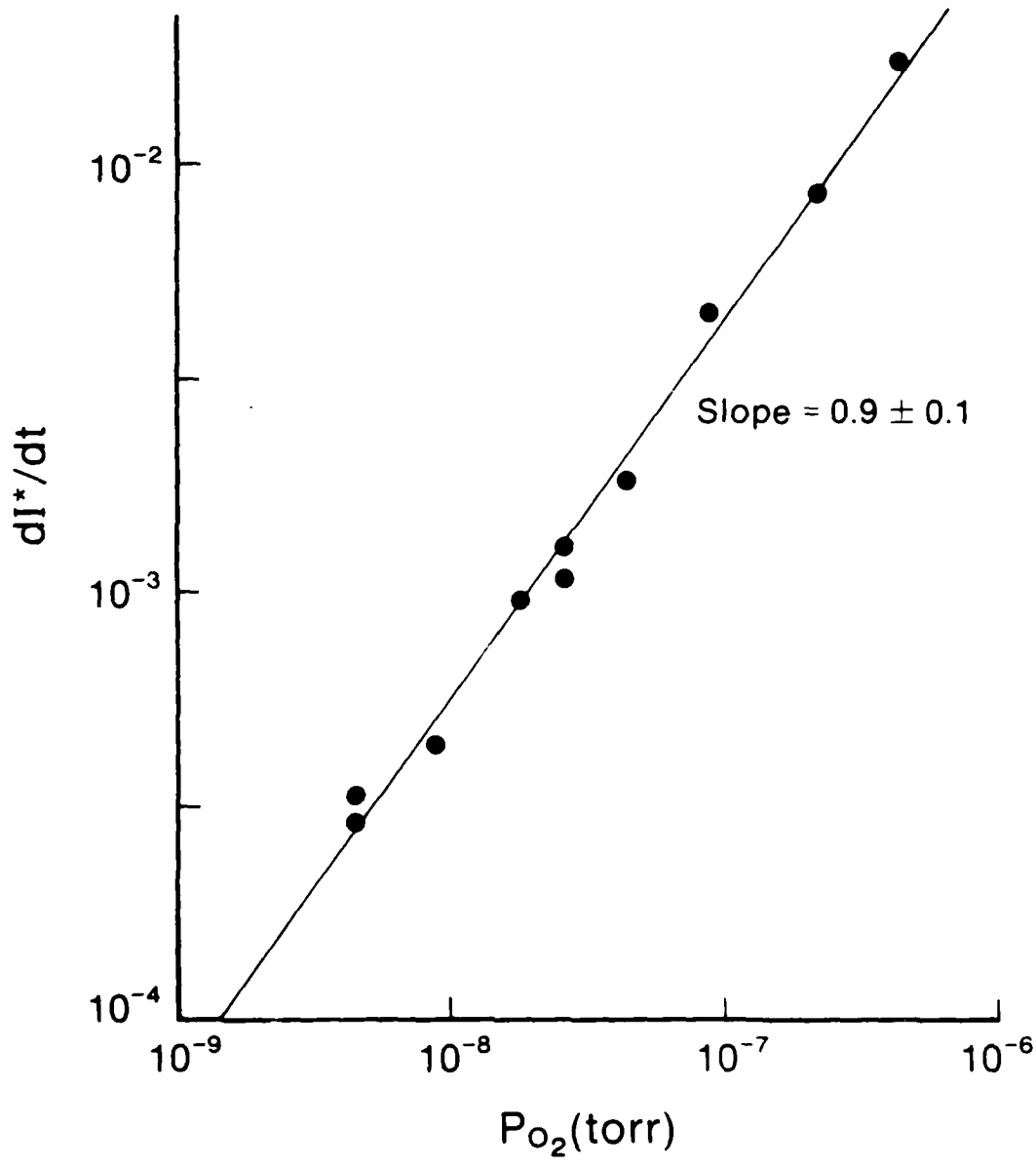
10^{-2}
10^{-3}
10^{-4}
dI^*/dt
Slope = 0.9 ± 0.1
10^{-9}
10^{-8}
10^{-7}
10^{-6}
P_{O_2}(torr)

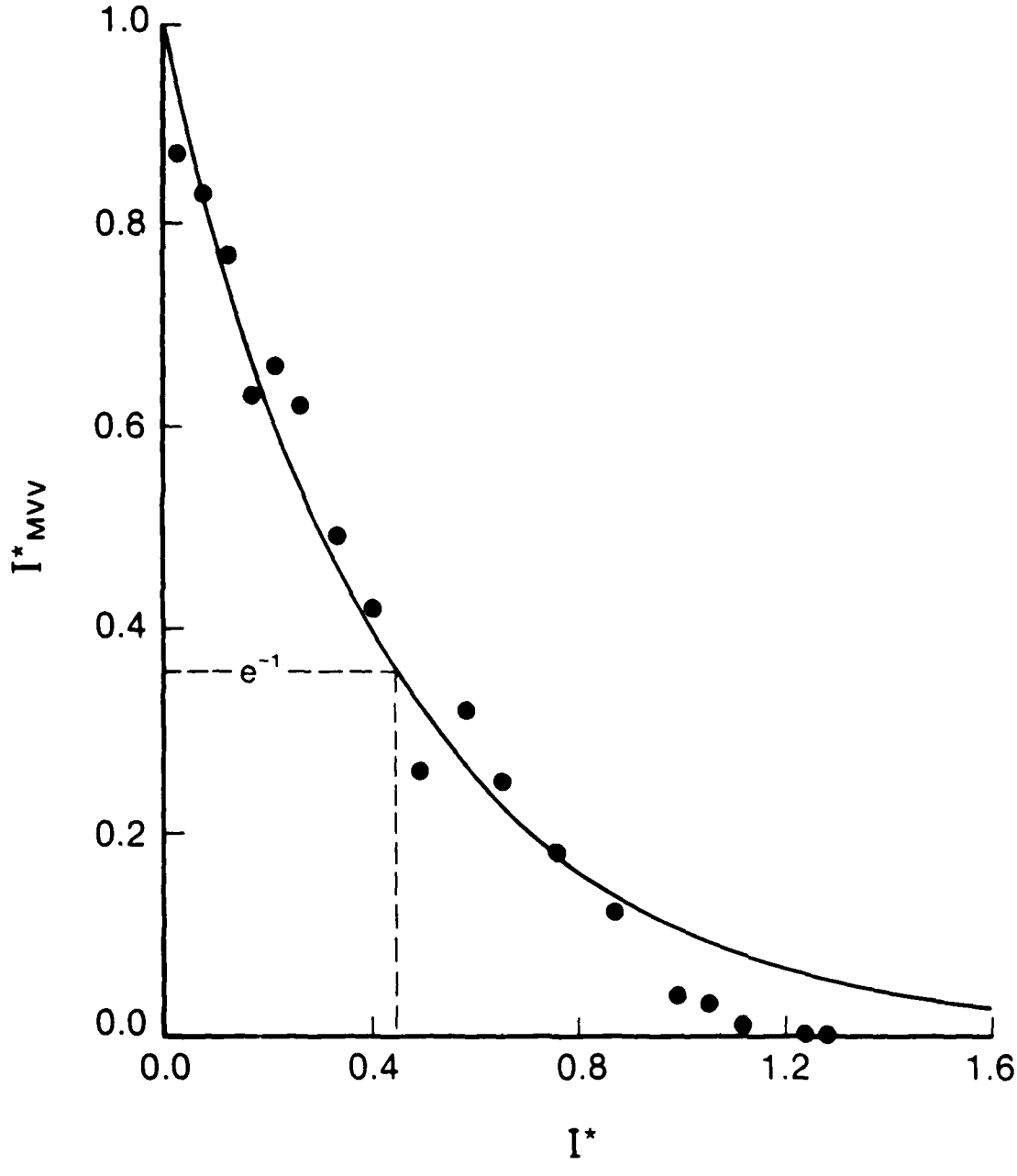
1.0
0.8
0.6
0.4
0.2
0.0
I^*_{MVV}
e^{-1}
0.0
0.4
0.8
1.2
1.6
I^*

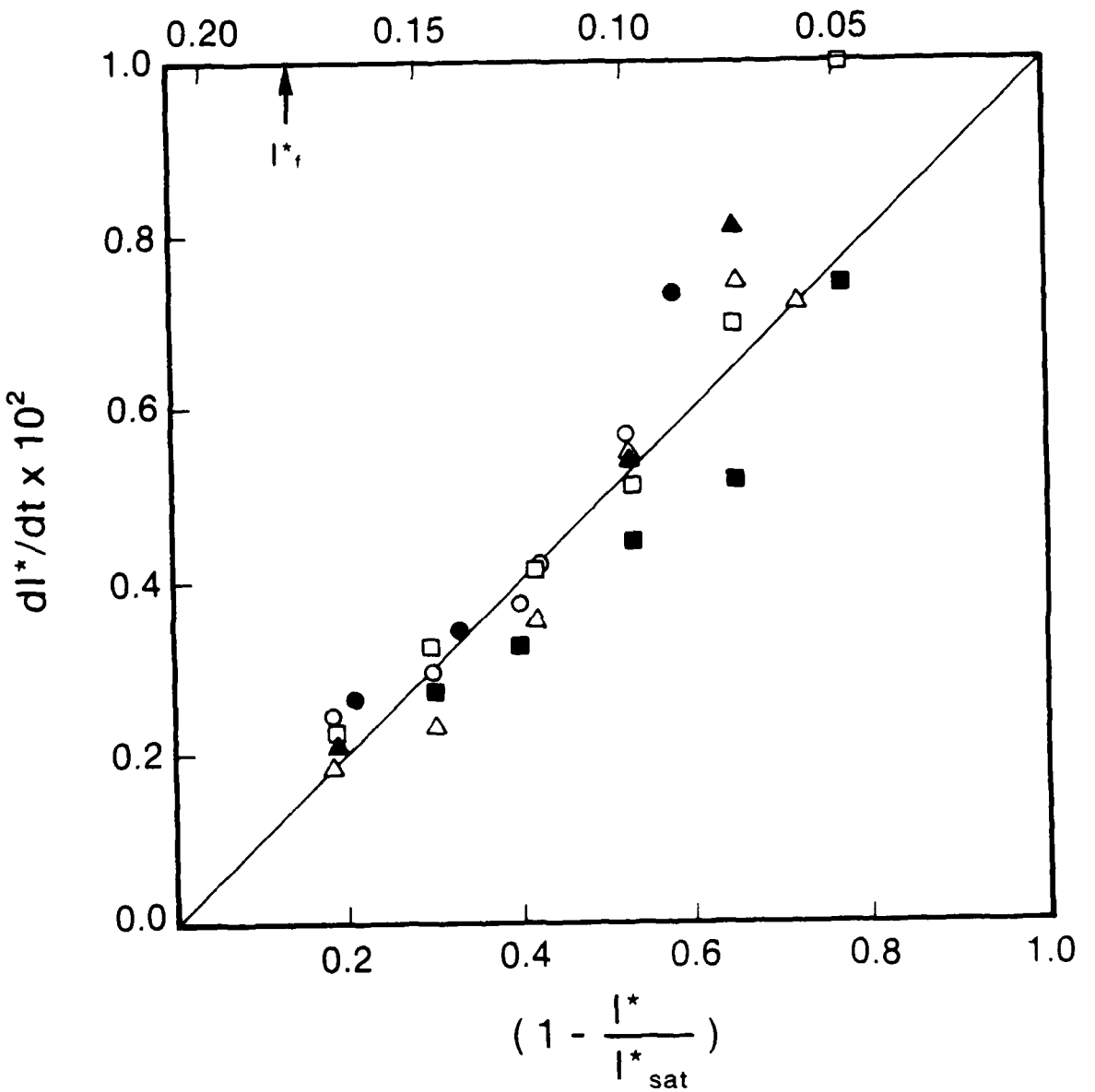
0.20
0.15
0.10
0.05
1.0
0.8
0.6
0.4
0.2
0.0
l^*_f
$dl^*/dt \times 10^2$
0.2
0.4
0.6
0.8
1.0
$(1 - \frac{l^*}{l^*_{sat}})$

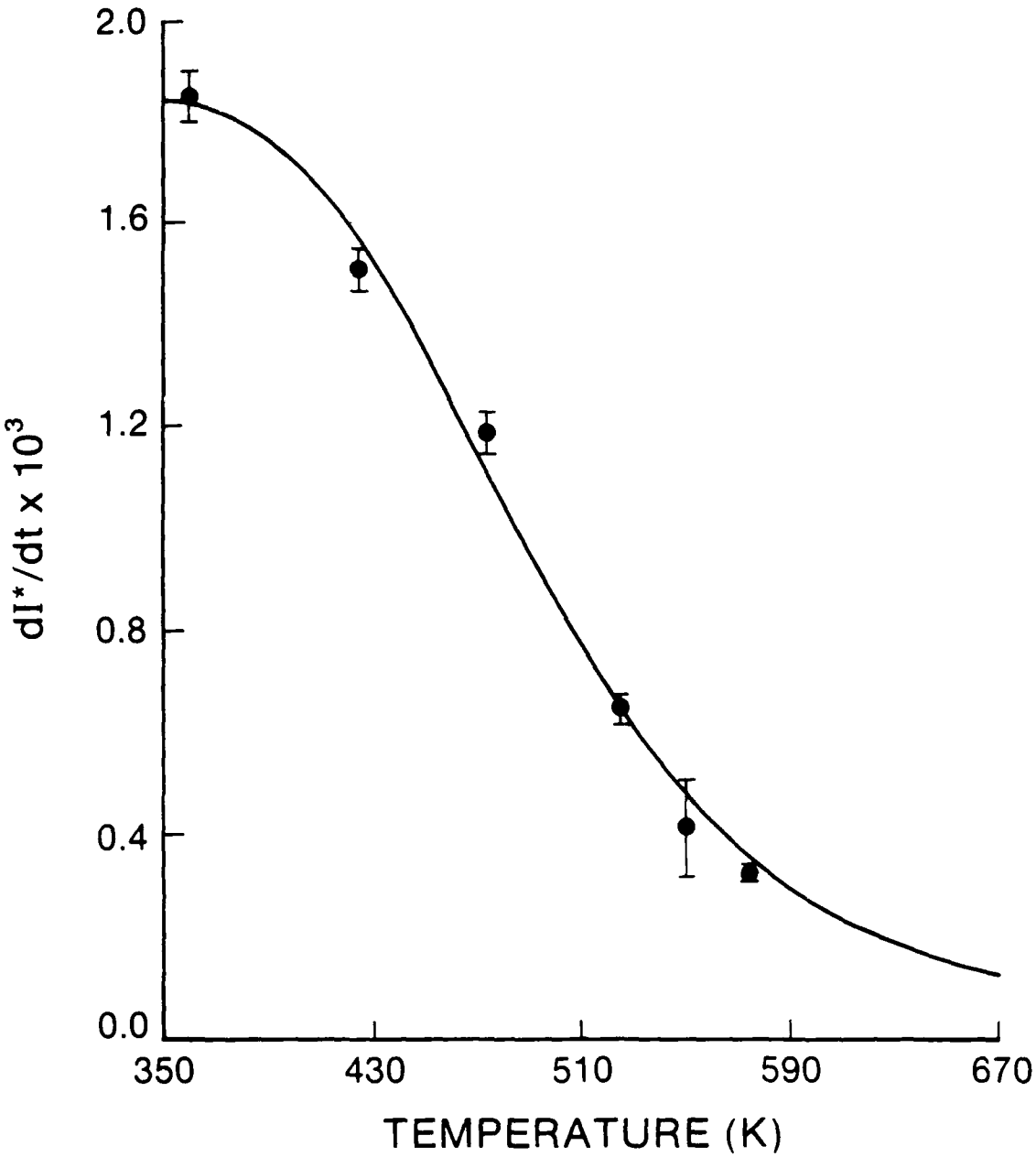
2.0
1.6
1.2
0.8
0.4
0.0
dI*/dt x 10³
350
430
510
590
670
TEMPERATURE (K)

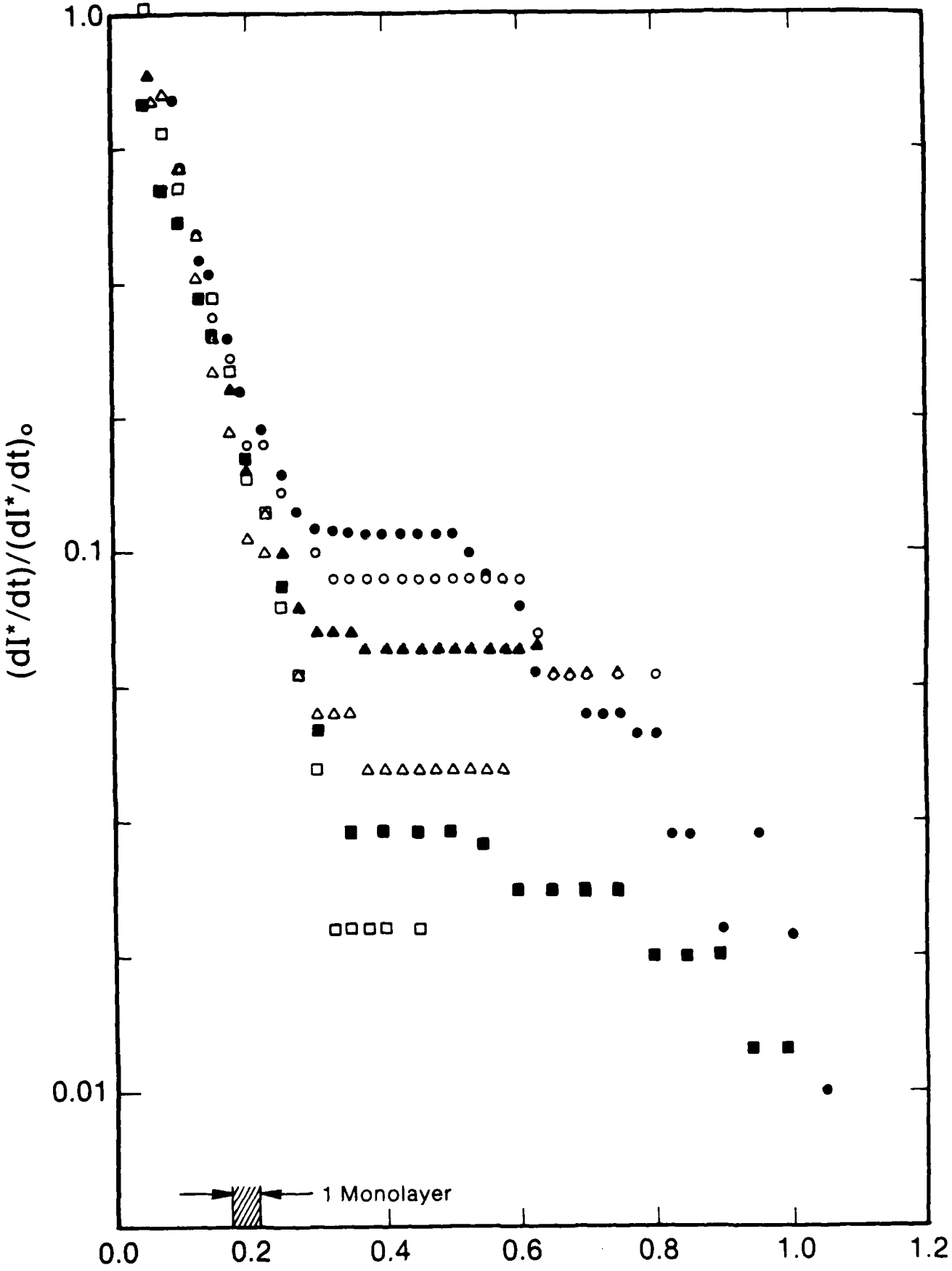
1.0
0.1
0.01
(dI*/dt)/(dI*/dt)o
1 Monolayer
0.0
0.2
0.4
0.6
0.8
1.0
1.2

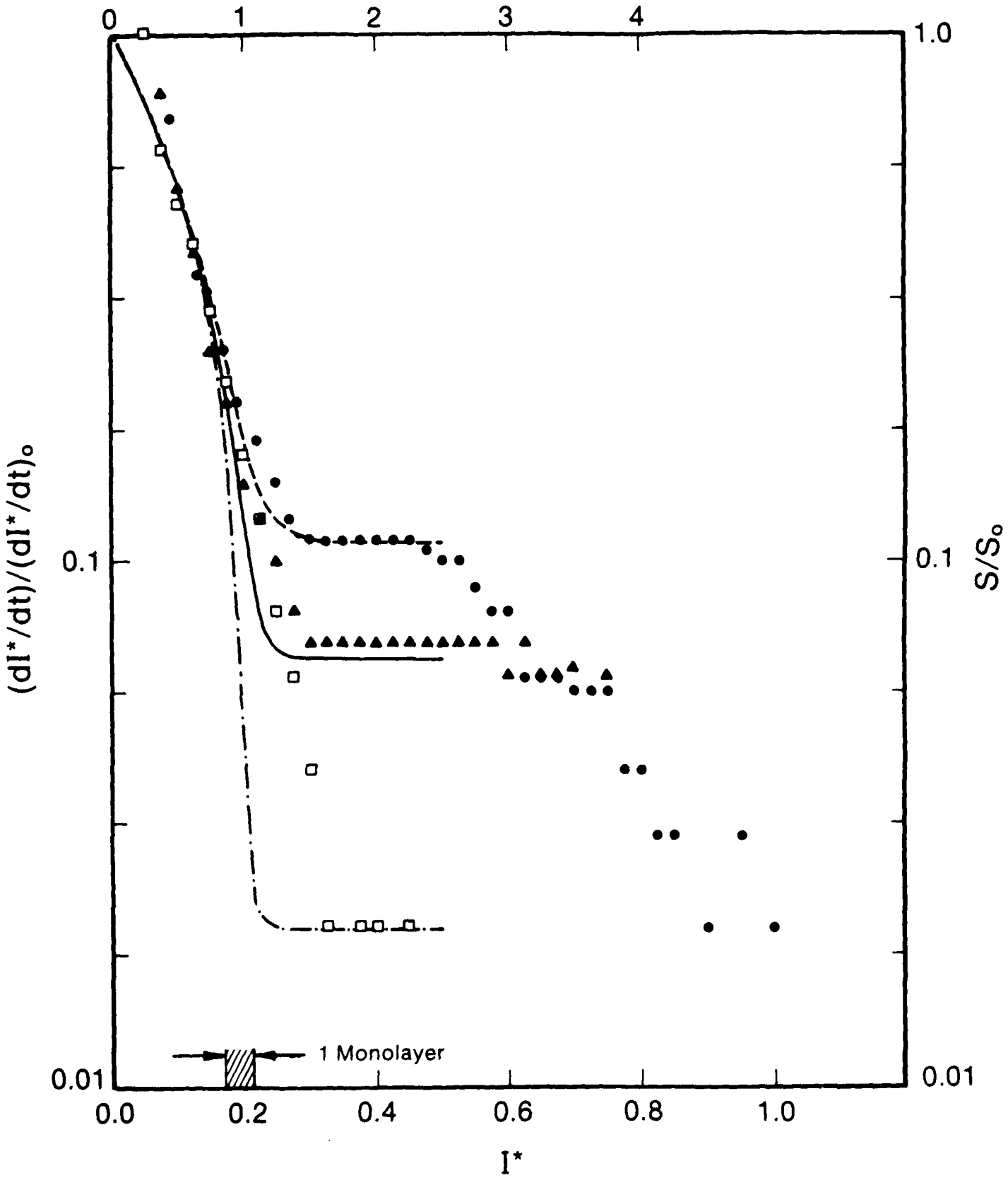
0
1
2
3
4
1.0
0.1
0.01
$(dI^*/dt)/(dI^*/dt)_o$
S/S_o
1 Monolayer
0.0
0.2
0.4
0.6
0.8
1.0
I^*